Analysis of the Effects of Operation Voltage Range in Flexible DC Control on Railway HPQC Compensation Capability in High-Speed Co-phase Railway Power

Keng-Weng Lao 🆔 , *Member, IEEE*, Man-Chung Wong, *Senior Member, IEEE*, Ningyi Dai, *Senior Member, IEEE*, Chi-Seng Lam, *Senior Member, IEEE*, Lei Wang, and Chi-Kong Wong, *Member, IEEE*

Abstract—Railway hybrid power quality conditioner (HPQC) is advantageous over conventional railway power quality conditioner (RPC) for its reduction in operation voltage and device ratings in co-phase traction power compensation. In order to further reduce the power loss during operation, flexible dc control has been proposed. However, the operation voltage range for railway HPQC has not yet been discussed. This is important since in contrast to traditional power quality compensation devices, active power compensation is involved in co-phase traction power. Compensation capability in co-phase traction power thus does refer not only to reactive power compensation but also to active power compensation ability. Satisfactory compensation performance can be provided only when railway HPQC can provide enough active and reactive compensation power output at the same time. In this paper, the effects of operation range in flexible dc voltage control on railway HPQC compensation capability is briefly discussed and analyzed. The analysis is verified via PSCAD simulations. A laboratory-scaled hardware prototype is also constructed to obtain experimental results for further verifications.

Index Terms—Co-phase traction power supply, flexible dc voltage control, high-speed railway, power quality, railway hybrid power quality conditioner (HPQC).

I. INTRODUCTION

IN ORDER to mitigate the power quality problems in power systems, researchers have been putting much effort to propose various power quality compensation devices [1]–[5]. These compensation devices are so important that the presence of power quality problems can lead to serious severe problems in some critical power systems. For example, in traction power supply system, the major power quality problems are system unbalance, reactive power, and harmonics [6]. Since the locomotive loadings can never be balanced among the two electric arms, this inject large amount of negative sequence current and cause unbalance problem, which threatens system stability. Furthermore, locomotive loadings are mostly inductive loadings, which draw lots of reactive power from the system source grid. This indicates inefficient energy usage and presence of reactive power, which will cause voltage stability problem. Moreover, usage of power electronic devices in locomotives introduces significant amount of harmonics in the system, which may cause additional heat and can damage the electronic components in the system. The system performance is satisfactory only when it satisfies certain standard imposed by the IEEE, the IEC, or the National standard [7], [8].

Traditionally, usage of special-made transformers such as impedance-matching balance, Scott and Wood-Bridge transformers, etc., is carried out to relieve the unbalance problem in traction power. However, it involves additional cost. Electrified railway contact wire sections may be connected in rotating turns to reduce the unbalance problem. However, these techniques cannot solve the unbalance problem completely and are not preferred. A shunt capacitor is traditionally used to solve the reactive power problem (1948) [9]. However, the compensation power is fixed, and it cannot provide dynamic performance. For the system reactive and harmonics problem, traditionally static var compensator (SVC) has been used as the solving technique in traction power [10]. However, the dynamic compensation performance of SVC is poor and it further injects harmonics into the system. Comparatively, compensation devices based on active devices such as static synchronous compensator (STATCOM) can provide better dynamic performances and unified solution of system unbalance and reactive power and harmonic problems simultaneously [11].

Co-phase traction power supply, whose typical structure is shown in Fig. 3, is one of the newly proposed supply system for high-speed electrified railway [12]–[17]. In contrast to the
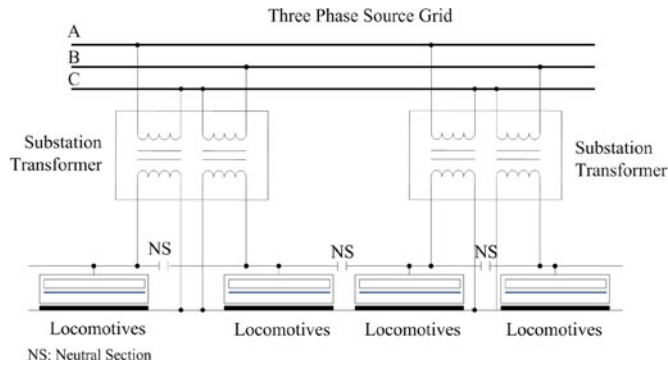
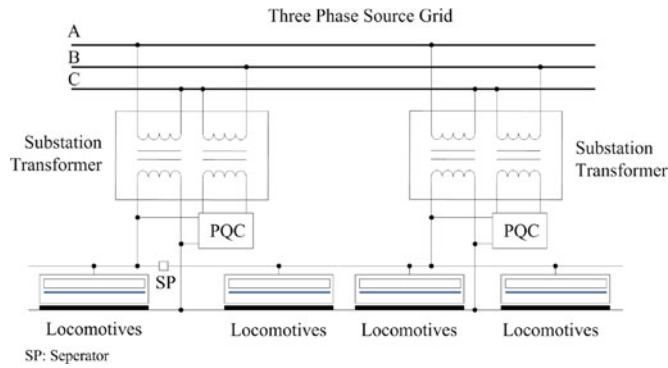Fig. 1.　Circuit topology of traditional traction power supply system.

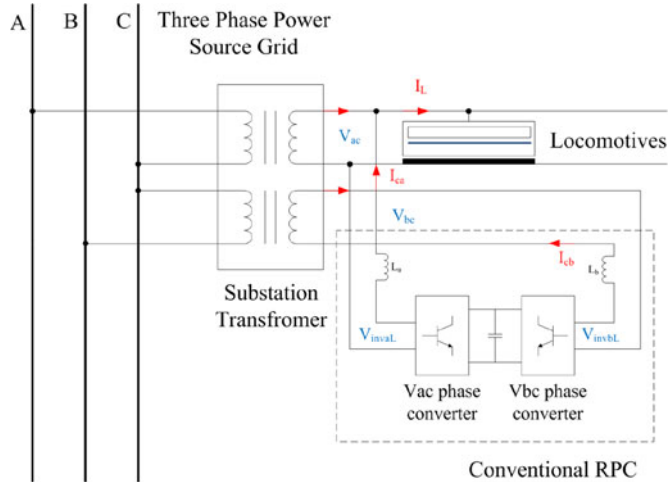Fig. 2.　Circuit topology of newly proposed co-phase traction power supply system.

Fig. 3.　Circuit schematics of co-phase traction power supply with conventional RPC.
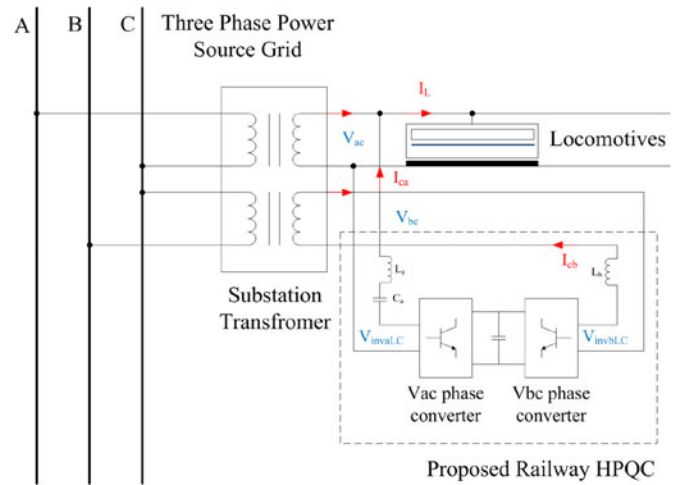

Fig. 4.　Circuit schematics of co-phase traction power supply with proposed railway HPQC.

quality problems mentioned and can enhance the power supply reliability as well as the transformer utilization ratio. In fact, the world's first co-phase device has already been put into trial operation in MeiShan substation in China [13].

As shown in Fig. 3, in traditional co-phase traction power, a two-phase railway power quality conditioner (RPC) is being used as PQC to provide power quality compensation from secondary to primary source grid. However, the inductive coupling structure of a two-phase RPC causes high operation voltage and lead to high initial cost and device rating.

Railway hybrid power quality conditioner (HPQC) is therefore proposed by our research group, in which a hybrid inductor–capacitor (*LC*) coupling structure is added in series with the compensator to reduce the operation voltage and device rating, so as to reduce the initial cost. The circuit schematics of the co-phase traction power supply with the newly proposed railway HPQC is shown in Fig. 4. Our working group has started relevant studies early in 2009, and the idea was first revealed to public in 2012 [18]. The parameter design of railway HPQC for a minimum operation voltage under nominal-rated load has then been developed and discussed (2013) [19]. The ratio allocation of coupled inductance and capacitance for a minimum operation voltage under harmonic compensation concern has also been explored [20]. The development of railway HPQC in previous studies mentioned earlier is developed based on steady loading condition. In order to make railway HPQC more suitable for practical cases, the relationship between railway HPQC operation voltage and loading condition is investigated [21]. Other relevant studies, including partial compensation of railway HPQC, have also been published [22]–[24]. However, the railway HPQC developed so far is based on fixed dc operation voltage. It has been verified that switching loss is directly proportional to dc voltage [25]. Excess unwanted power loss will be resulted since sometimes lower operation voltage is required when load condition varies. Flexible dc control algorithm was then proposed for power quality conditioning devices [26]. Nevertheless, the analysis is not completely applicable since

traditional traction power supply (shown in Fig. 1), locomotive loadings are connected across one single-phase output of the substation transformer (as shown in Fig. 2). The structure is advantageous than the quantity of neutral sections (NS) (for isolating two different electric arm phase outputs) can be effectively eliminated. This allows locomotives to reach higher speed since they lose power and velocity when passing through NSs (when they are present). Moreover, the power quality compensation (PQC) device in the system can help to solve the power

active power compensation is involved in co-phase traction power and railway HPQC, which makes the application different from other power quality compensation.

In order to enhance the performance, different control techniques have been proposed for railway power quality compensators. For example, in [28], a dual-loop control strategy based on fuzzy algorithm is proposed for RPC to suppress the dc-link voltage fluctuation and enhance the RPC stability. In [29], a strategy of negative sequence and harmonic current compensation in RPC is proposed. In [30], the parameter design and control of RPC, coupled with asymmetric double *LC* branches, are briefly discussed and analyzed. In [31], a modified negative-sequence current optimizing control is proposed to enhance the system performance to optimize the compensation power. However, in the studies mentioned earlier, the focus of the control is mainly to maintain a stable dc-link voltage. With a fixed dc-link voltage, the compensation performance will degrade when the loading condition goes beyond the compensation range of the compensator. This problem can be overcome when the dc-link voltage is allowed to change according to the loading condition.

In this paper, a flexible dc voltage control is proposed and the effect of operation range in flexible dc voltage control on the railway HPQC compensation capability is analyzed. The operation voltage range is determined by comparing the railway HPQC compensation power output region (based on dc voltage) and the desired compensation range. The operation voltage reference can then be selected based on the loading operation condition, and the dc voltage can be tracked using traditional P or PI control. In order to achieve this, a complete analysis of the railway HPQC compensation power with the dc link voltage, as well as the compensation range, is required. In Section I, a brief introduction about motivation of the research study is introduced. In Section II, the variation of output active and reactive power range caused by the dc operation voltage range in the railway HPQC is introduced and discussed. The compensation capability of railway HPQC can then be determined by solving (19). Relevant details are provided in Section III. The effect of variation in the operation range in flexible dc voltage control on the compensation capability is then explored and discussed based on the analysis in the previous sections. Finally, in Section IV, simulation and experimental verifications obtained from laboratory hardware prototype are presented to verify system performance. A summary of the paper contents is then concluded in Section V.

II. EFFECT OF FLEXIBLE DC VOLTAGE CONTROL OPERATION RANGE ON RAILWAY HPQC OUTPUT ACTIVE AND REACTIVE POWER OUTPUT CAPABILITY

As discussed, the main function of railway HPQC is to output active and reactive power from the traction secondary side to source grid to provide power quality compensation in the co-phase traction power. When the operation voltage is varied, the railway HPQC active and reactive power output capability is also varied. The railway HPQC output power capability is directly related to its compensation capability. Therefore, the re-
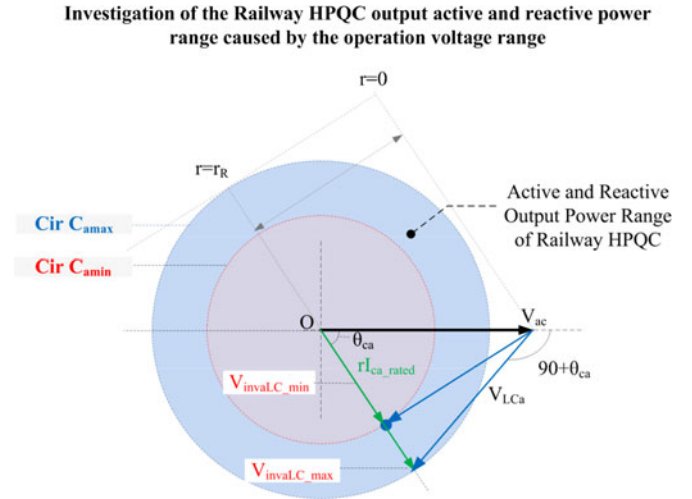

Fig. 5. Vector diagram showing operation of railway HPQC in co-phase traction power supply (output power range and compensation requirement).

lationship between the operation voltage range and the railway HPQC active and reactive power output capability is discussed.

As indicated in Section I, the railway HPQC is composed of two single-phase converters with back-to-back connection. In this paper, the analysis is performed based on the assumption that the railway HPQC operation voltage is dominant by the V_{ac} phase converter. In other words, the operation voltage requirement of V_{ac} phase converter is always larger than that of V_{bc} phase converter [19]. This may be achieved by selecting appropriate turning ratio of the transformer, which the V_{bc} phase converter is connected to, as well as through appropriate design of V_{bc} phase converter. Therefore, analysis is mainly performed in the V_{ac} phase converter in this paper. Assuming that the railway HPQC V_{ac} phase inverter output is V_{invaLC}, the expression in (1) can be obtained by performing circuit analysis shown in Fig. 4

$$\bar{V}_{\mathrm{invaLC}} = \bar{V}_{\mathrm{ac}} + \bar{V}_{\mathrm{LC}a} = \bar{V}_{\mathrm{ac}} + \bar{I}_{\mathrm{ca}}\bar{X}_{\mathrm{LC}a} \qquad (1)$$

where V_{invaLC} is the inverter output voltage of the railway HPQC V_{ac} phase converter, V_{ac} is the PCC voltage at the V_{ac} phase, $V_{\mathrm{LC}a}$ is the voltage drop across the coupled impedance of the railway HPQC, and I_{ca} is the V_{ac} phase converter output compensation current.

Fig. 5 depicts a vector diagram showing the active and reactive power output range of the railway HPQC for power quality compensation in co-phase traction power supply based on (1).

Satisfactory compensation performance can be obtained whenever the edge of the vector $V_{\mathrm{LC}a}$ (voltage across the hybrid coupled structure) is located at the area bounded by the circle with the radius of operation voltage (V_{invaLC}). It is assumed that the operation voltage range of railway HPQC is from $V_{\mathrm{invaLC}_{\min}}$ to $V_{\mathrm{invaLC}_{\max}}$. As shown in Fig. 5, the active and reactive power output range of railway HPQC is determined by the circle $C_{a\max}$, which has the maximum operation voltage $V_{\mathrm{invaLC}_{\max}}$ within the operation range. The mathematical relationship can be derived from Fig. 5. Supposing that the operation voltage of the railway HPQC is V_{invaLC} (where

$V_{\mathrm{invaLC_{min}}} < V_{\mathrm{invaLC}} < V_{\mathrm{invaLC_{max}}}$, with the railway HPQC output current composing of active and reactive parts, the current I_{ca} can be expressed as in (2), while the expression for vector V_{invaLC} in (3) can be obtained by substituting (2) into (1). Finally, the magnitude of the railway HPQC V_{invaLC} can then be determined by (4), by trigonometric relationship

$$\bar{I}_{\mathrm{ca}} = I_{\mathrm{cap}} - jI_{\mathrm{caq}} \qquad (2)$$

$$\bar{V}_{\mathrm{invaLC}} = (V_{\mathrm{ac}} - I_{\mathrm{caq}} \cdot X_{\mathrm{LC}a}) - j\left(I_{\mathrm{cap}} \cdot X_{\mathrm{LC}a}\right) \qquad (3)$$

$$\left|\bar{V}_{\mathrm{invaLC}}\right| = \sqrt{(V_{\mathrm{ac}} - I_{\mathrm{caq}} \cdot X_{\mathrm{LC}a})^2 + (I_{\mathrm{cap}} \cdot X_{\mathrm{LC}a})^2} \qquad (4)$$

where I_{caq} is the reactive portion of the V_{ac} phase converter compensation current and I_{cap} is the active portion of the V_{ac} phase converter compensation current.

In order to simplify the analysis, the following definitions and assumptions are made for the coupled impedance $X_{\mathrm{LC}a}$, as well as the railway HPQC output active (p_{ca}) and reactive (q_{ca}) power, as shown in (5), (6), and (7). These assumptions are useful to eliminate some parameters during analysis in the following derivations:

$$X_{\mathrm{LC}a} = m_{\mathrm{LC}a} \cdot \left(\frac{V_{\mathrm{ac}}}{I_{\mathrm{ca\_rated}}}\right) \qquad (5)$$

$$s_{\mathrm{HPQC\_rated}} = V_{\mathrm{ac}} \cdot I_{\mathrm{ca\_rated}} \qquad (6)$$

$$p_{\mathrm{ca}} = V_{\mathrm{ac}} I_{\mathrm{cap}}$$

$$q_{\mathrm{ca}} = V_{\mathrm{ac}} I_{\mathrm{caq}}. \qquad (7)$$

By substituting (5), (6), and (7) into (4), the expressions in (16) can be obtained. For simplicity, the railway HPQC operation voltage V_{invaLC} is expressed as a ratio of the point of common coupling (PCC) voltage V_{ac} as the operation voltage rating k_{invaLC}. Moreover, the equal sign is replaced by the "larger than" sign in order to describe the shaded region (railway HPQC active and reactive power output range) in Fig. 6, eq. (8) shown at the bottom f this page, where p_{ca} is the active compensation power output from the railway HPQC V_{ac} phase converter, p_{ca} is the reactive compensation power output from the railway HPQC V_{ac} phase converter, and $I_{\mathrm{ca\_rated}}$ is the rated compensation current (at a designed value).

By further manipulation of (7), the expression can be rearranged as shown in (9). The value of $s_{\mathrm{HPQC\_rated}}$ is fixed since the railway HPQC coupled impedance and the PCC voltage do not change. Therefore, the expression shows that the relationship between the railway HPQC output active and re-
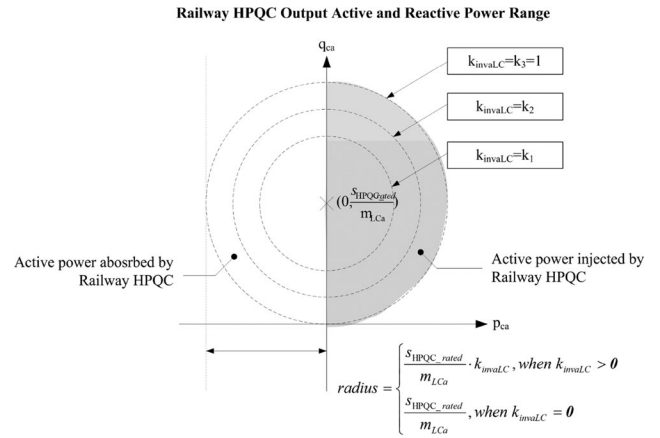

Fig. 6. Railway HPQC output active and reactive power range bounded by different circles under different operation voltage ratings k_{invaLC}.

active power range, p_{ca} and q_{ca}, forms different circles under different operation voltage rating k_{invaLC}. These circles are different from the circle C_{a1} in (9)

$$\left(\frac{p_{\mathrm{ca}}}{\frac{s_{\mathrm{HPQC\_rated}}}{m_{\mathrm{LC}a}}}\right)^2 + \left(\frac{\frac{s_{\mathrm{HPQC\_rated}}}{m_{\mathrm{LC}a}} - q_{\mathrm{ca}}}{\frac{s_{\mathrm{HPQC\_rated}}}{m_{\mathrm{LC}a}} \cdot k_{\mathrm{invaLC}}}\right)^2 \le 1. \qquad (9)$$

Therefore, according to the conclusion drawn earlier that the railway HPQC active and reactive power output range is determined by the maximum operation voltage $V_{\mathrm{invaLC_{max}}}$, the expression in (9) may be revised as (10)

$$\left(\frac{p_{\mathrm{ca}}}{\frac{s_{\mathrm{HPQC\_rated}}}{m_{\mathrm{LC}a}}}\right)^2 + \left(\frac{\frac{s_{\mathrm{HPQC\_rated}}}{m_{\mathrm{LC}a}} - q_{\mathrm{ca}}}{\frac{s_{\mathrm{HPQC\_rated}}}{m_{\mathrm{LC}a}} \cdot k_{\mathrm{invaLC\_max}}}\right)^2 \le 1. \qquad (10)$$

By investigating the expression in (9), the center of the described circle is at $(0, s_{\mathrm{rated}}/m_{\mathrm{LC}a})$ and the corresponding radius is $(s_{\mathrm{HPQC\_rated}})(k_{\mathrm{invaLC}})/m_{\mathrm{LC}a}$. The graphical representation is shown in Fig. 6.

For instance, assuming the traction load power factor value of 0.85 and the railway HPQC coupled impedance design $m_{\mathrm{LC}a} = 0.87$ (based on the rated load) and $s_{\mathrm{HPQC\_rated}} = 1.0$, the variation of output active and reactive power is shown in Fig. 7.

Many important points can be inferred from the figures, including, but not limited to:

1) With a higher value of railway HPQC operation voltage rating k_{invaLC}, the range of the railway HPQC output active and reactive power is also higher.

$$V_{\mathrm{invaLC}} \ge \sqrt{\left(V_{\mathrm{ac}} - V_{\mathrm{ac}} \cdot (V_{\mathrm{ac}} I_{\mathrm{caq}}) \cdot \frac{m_{\mathrm{LC}a}}{V_{\mathrm{ac}} I_{\mathrm{ca\_rated}}}\right)^2 + \left(V_{\mathrm{ac}} \cdot (V_{\mathrm{ac}} I_{\mathrm{cap}}) \cdot \frac{m_{\mathrm{LC}a}}{V_{\mathrm{ac}} I_{\mathrm{ca\_rated}}}\right)^2}$$

$$\frac{V_{\mathrm{invaLC}}}{V_{\mathrm{ac}}} \ge \sqrt{\left(1 - q_{\mathrm{ca}} \cdot \frac{m_{\mathrm{LC}a}}{s_{\mathrm{HPQC\_rated}}}\right)^2 + \left(p_{\mathrm{ca}} \cdot \frac{m_{\mathrm{LC}a}}{s_{\mathrm{HPQC\_rated}}}\right)^2}$$

$$k_{\mathrm{invaLC}} \ge \sqrt{\left(1 - q_{\mathrm{ca}} \cdot \frac{m_{\mathrm{LC}a}}{s_{\mathrm{HPQC\_rated}}}\right)^2 + \left(p_{\mathrm{ca}} \cdot \frac{m_{\mathrm{LC}a}}{s_{\mathrm{HPQC\_rated}}}\right)^2} \qquad (8)$$
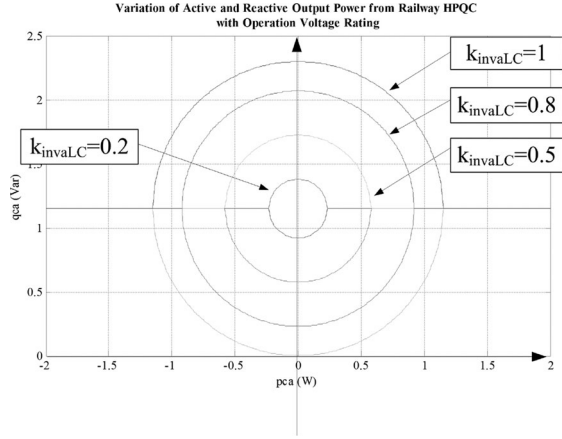
Fig. 7. MATLAB plot constructed based on railway HPQC impedance design $m_{\mathrm{LC}a} = 0.87$ under different operation voltage ratings.

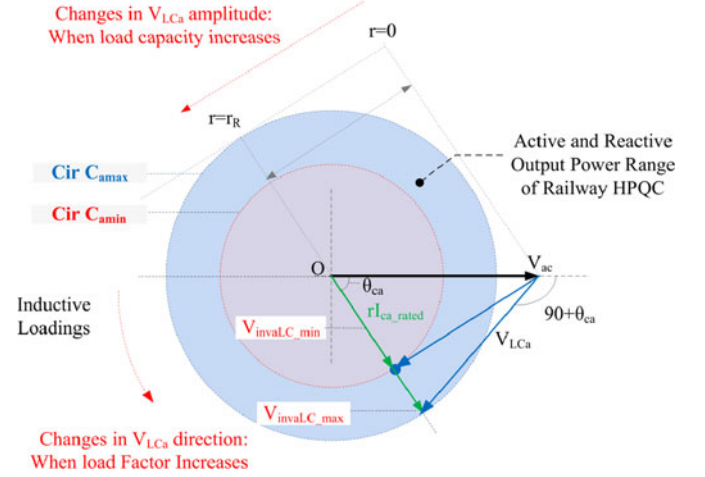

Fig. 8. Vector diagram showing the variation of active and reactive compensation power requirement when load condition varies.

2) The middle point of the range in the reactive power output is always located at $s_{\mathrm{HPQC\_rated}}/m_{\mathrm{LC}a}$.

3) With certain railway HPQC operation voltage rating (k_{invaLC} not equal to 0), the railway HPQC may be used to inject or absorb the active power.

4) When the value of k_{invaLC} is 0.0, the railway HPQC can provide reactive power compensation only with amount of $s_{\mathrm{HPQC\_rated}}/m_{\mathrm{LC}a}$.

5) When the value of k_{invaLC} is 1.0, the range of reactive power compensation goes from 0 to $(s2_{\mathrm{HPQC\_rated}})/m_{\mathrm{LC}a}$, but no active power can be injected into the system at these two boundaries.

To conclude, based on the discussions above, the railway HPQC active and reactive power output range is mainly determined by the maximum value of the dc operation voltage range ($V_{\mathrm{invaLC_{max}}}$) and can be determined by (10).

III. EFFECT OF FLEXIBLE DC VOLTAGE CONTROL OPERATION RANGE ON RAILWAY HPQC COMPENSATION CAPABILITY IN CO-PHASE TRACTION POWER SUPPLY

In Section II, the effect of railway HPQC operation voltage range on its active and reactive power output range is briefly discussed. As indicated in Introduction, the ultimate goal is to explore the effect of flexible DC voltage control operation range on railway HPQC compensation capability in co-phase traction power. However, the compensation capability of railway HPQC is not only determined by active and reactive output only. It is also dependent on the compensation requirement of co-phase traction power supply since there is a certain relationship between the required active and reactive compensation power.

The compensation power requirement of the co-phase traction power railway HPQC can be derived based on the power quality requirement and is shown in (11) [23], [24]. Detailed derivation procedures can be found in the reference and will not be discussed here

$$\begin{cases} p_{\mathrm{ca}} = K_1 \bar{p}_L \\ q_{\mathrm{ca}} = K_2 \bar{p}_L + \tilde{p}_L + K_3 q_L \\ p_{\mathrm{cb}} = -K_1 \bar{p}_L \\ q_{\mathrm{cb}} = -K_2 \bar{p}_L \end{cases} \quad (11)$$

where p_{ca}, p_{cb} refer to the active power requirement of V_{ac} phase and V_{bc} phase converters, respectively; q_{ca} and q_{cb} refer to the reactive power requirement of V_{ac} phase and V_{bc} phase converters, respectively, in railway HPQC; and $\bar{p}_L$ refers to the dc portion of the instantaneous load active power, while q_L refers to the instantaneous load reactive power. Under ideal compensation, $K_1 = 0.5$, $K_2 = 0.2887$, and $K_3 = 1.0$.

A. Changes in Railway HPQC Compensation Requirement When the Load Condition Changes

First, it should be noticed that when the edge of $V_{\mathrm{LC}a}$ is located outside the shaded area in Fig. 5, railway HPQC cannot provide satisfactory performance. This thus indicates the limitation of railway HPQC compensation in the co-phase traction power.

Fig. 8 depicts a vector diagram showing the variation of compensation requirement when the load condition changes. Basically, the railway HPQC is designed based on the rated value, and normally, its hardware will not be changed.

When load condition varies, both load capacity and load power factor may vary. In the discussions below, the changes in vector $V_{\mathrm{LC}a}$ and compensation power requirement due to variations in load capacity and load power factor are studied respectively.

1) Changes Due to Variations in Load Capacity: First, the changes due to variations in load capacity are being investigated. According to (11), when the load capacity increases, IL increases such that the compensation power p_{ca} and q_{ca} also increase. This results in the increase in the compensation current across the hybrid coupled structure and causes larger voltage drop $V_{\mathrm{LC}a}$. The amplitude of $V_{\mathrm{LC}a}$ will then get larger when the load capacity increases. This is expressed in Fig. 8.

Next, the changes in the railway HPQC active and reactive compensation power requirement due to changes in load capacity can then be explored. A new parameter r (per unit of rated

load) is introduced to model the load capacity variation. Assuming that the rated fundamental active and reactive compensation power based on the designed rated load is defined as in (12), when the load capacity varies to r times of the rated value, the required active and reactive compensation power also change to r times of the rated ones, as shown in (13). The required active and reactive compensation power output of railway HPQC is therefore directly proportional to the load capacity variations r

$$\begin{cases} p_{\text{ca\_rated}} = K_1 \left(\bar{p}_{L\_\text{rated}} \right) \\ q_{\text{ca\_rated}} = K_2 \left(\bar{p}_{L\_\text{rated}} \right) + K_3 \left(q_{L\_\text{rated}} \right) \\ p_{\text{cb\_rated}} = -K_1 \left(\bar{p}_{L\_\text{rated}} \right) \\ q_{\text{cb\_rated}} = -K_2 \left(\bar{p}_{L\_\text{rated}} \right) \end{cases} \tag{12}$$

$$\begin{cases} p_{\text{ca}} = K_1 \left(r\bar{p}_{L\_\text{rated}} \right) = rp_{\text{ca\_rated}} \\ q_{\text{ca}} = K_2 \left(r\bar{p}_{L\_\text{rated}} \right) + K_3 \left(rq_{L\_\text{rated}} \right) = rq_{\text{ca\_rated}} \\ p_{\text{cb}} = -K_1 \left(r\bar{p}_{L\_\text{rated}} \right) = rp_{\text{cb\_rated}} \\ q_{\text{cb}} = -K_2 \left(r\bar{p}_{L\_\text{rated}} \right) = rq_{\text{cb\_rated}} \end{cases} . \tag{13}$$

It is further defined that the required apparent compensation power at the rated load is $s_{L_{\text{rated}}}$ such that it follows the relationship in (14), when the load capacity is changed to r p.u., the relationship between r, p_{ca}, and q_{ca} can be then be obtained as in (15)

$$\left(p_{\text{ca\_rated}} \right)^2 + \left(q_{\text{ca\_rated}} \right)^2 = \left(s_{L\_\text{rated}} \right)^2 \tag{14}$$

$$\left(p_{\text{ca}} \right)^2 + \left(q_{\text{ca}} \right)^2 = \left(rp_{\text{ca\_rated}} \right)^2 + \left(rq_{\text{ca\_rated}} \right)^2 = \left(rs_{L\_\text{rated}} \right)^2 . \tag{15}$$

The expression in (15) shows that the required active and reactive power requirement of railway HPQC due to load variations is defined by circles centered at origin, with radius of rs_{L_rated}.

2) Changes Due to Variations in Load Power Factor: Besides load capacity, the load power factor may also vary during load variations. Referring to (11), it can be observed that as the load power factor varies, the required compensation power also changes. By further manipulation, the expression in (16) can be obtained, where PF_L refers to the load power factor

$$\begin{cases} p_{\text{ca}} = 0.5\bar{p}_L = 0.5 \left(\text{PF}_L \right) \left(I_L \right) \left(V_{\text{ac}} \right) = 0.5 \left(PF_L \right) \left(s_L \right) \\ q_{\text{ca}} = 0.2887\bar{p}_L + q_L \\ \quad = \left[0.2887 \left(\text{PF}_L \right) + \sqrt{1 - \left(\text{PF}_L \right)^2} \right] \left(I_L \right) \left(V_{\text{ac}} \right) \\ \quad = \left[0.2887 \left(\text{PF}_L \right) + \sqrt{1 - \left(\text{PF}_L \right)^2} \right] \left(s_L \right) . \end{cases} \tag{16}$$

By eliminating the value of s_L in (16), the ratio between the required active and reactive power output from railway HPQC in co-phase traction power shown in (17) can be obtained. This relationship is a special co-phase traction power railway HPQC compensation and makes the investigation unique

$$\frac{q_{\text{ca}}}{p_{\text{ca}}} = \left\{ \frac{2 \cdot \left[0.2887 \left(\text{PF}_L \right) + \sqrt{1 - \left(\text{PF}_L \right)^2} \right]}{\text{PF}_L} \right\} \tag{17}$$
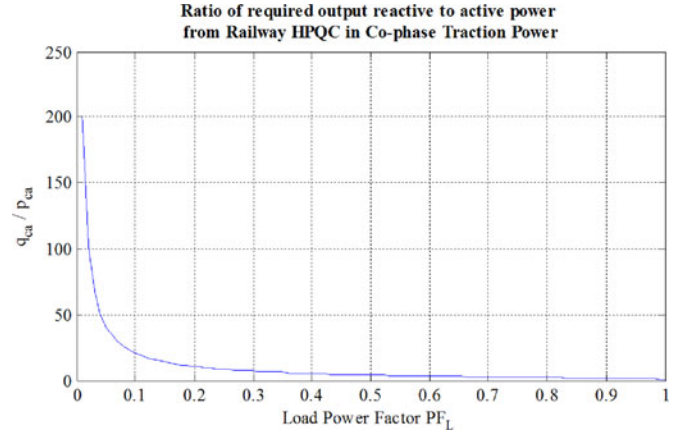

Fig. 9. MATLAB plot showing the variation of railway HPQC output reactive to active requirement in co-phase traction power with load power factor PF_L.

where PF_L is the load power factor.

It can be observed from the expression that the ratio of q_{ca} to p_{ca} is a function of the load power factor PF_L. A MATLAB plot is being constructed according to (17) and is shown in Fig. 9. The relationship between them is not linear. With the load power factor $= 0$, the amount of required output reactive power q_{ca} is higher. As the load power factor increases, the ratio decreases. For instance, for the load power factor $= 0.85$, the ratio $q_{\text{ca}}/p_{\text{ca}}$ is 1.82. This ratio further limits the required railway HPQC compensation power range.

3) Changes Due to Variations in Both Load Capacity and Power Factor: In the discussions given later, the changes in railway HPQC active and reactive power due to variations in both load capacity and load power factor are explored. This can be done so by investigating (15) and (17), which is shown together as follows:

$$\begin{cases} \left(p_{\text{ca}} \right)^2 + \left(q_{\text{ca}} \right)^2 = \left(rs_{L\_\text{rated}} \right)^2 \\ \dfrac{q_{\text{ca}}}{p_{\text{ca}}} = \left\{ \dfrac{2 \cdot \left[0.2887 \left(\text{PF}_L \right) + \sqrt{1 - \left(\text{PF}_L \right)^2} \right]}{\text{PF}_L} \right\} \end{cases} . \tag{18}$$

The expressions in (18) are plotted in Fig. 10 under different load power factor PF_L and capacity variation r. The required compensation active and reactive power is unique under certain values of load power factor PF_L and load capacity r (p.u.), which can be determined by the intersection of the circle (caused by the load capacity variation) and the line (caused by the load power factor variation). It can be seen that first as the load capacity varies, the radius of the circle increases with the center at origin (0,0), while when the load power factor increases, the line rotates clockwise about the origin (0,0). It can also be seen that when the load power factor is fixed, the ratio between q_{ca} and p_{ca} is also a constant. For example, with the load power factor value of 0.85 and the capacity value of 1.2 p.u., the only possible railway HPQC active and reactive power output is located at point X (0.58, 1.06) in Fig. 10.
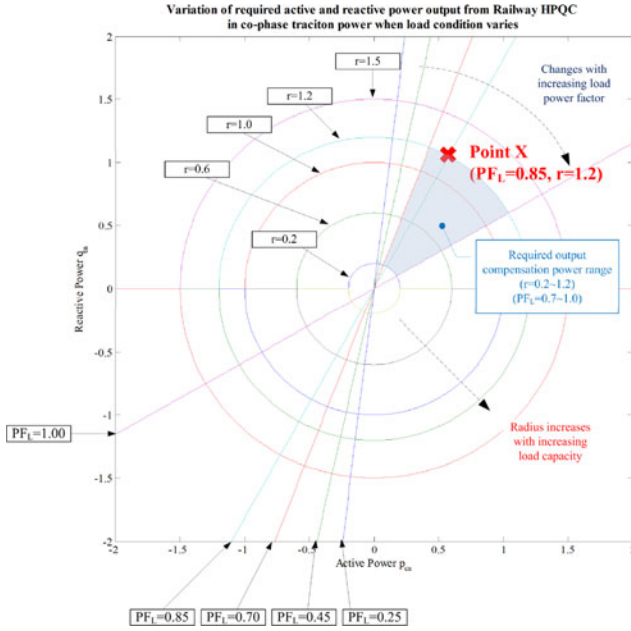
Fig. 10. MATLAB plot showing the variation of railway HPQC active and reactive power output requirement with changes in loading condition (load capacity and load power factor).

Furthermore, assuming that the traction load capacity varies from $r = 0.2$ to 1.2 and the load power factor varies from 0.7 to 1.0, the required compensation power range would be bounded by the lines and circles, shown as shaded area in Fig. 10. Satisfactory compensation performance can be provided by railway HPQC during these variations only when the railway HPQC output range covers this shaded region.

4) Effect of Railway HPQC Operation Range on Compensation Capability: Assuming that the operation voltage of railway HPQC is from $k_{\text{invaLC}_{\min}}$ to $k_{\text{invaLC}_{\max}}$, satisfactory compensation performance can be provided when the condition in (19) is satisfied

$$
\begin{cases}
(p_{\text{ca}})^2 + (q_{\text{ca}})^2 = (r s_{L\_\text{rated}})^2 \\
\dfrac{q_{\text{ca}}}{p_{\text{ca}}} = \left\{ \dfrac{2 \cdot \left[0.2887 \left(\text{PF}_L \right) + \sqrt{1 - \left(\text{PF}_L \right)^2} \right]}{\text{PF}_L} \right\} = M \\
k_{\text{invaLC}} = \sqrt{\left(1 - q_{\text{ca}} \cdot \dfrac{m_{LCa}}{s_{\text{HPQC\_rated}}} \right)^2 + \left(p_{\text{ca}} \cdot \dfrac{m_{LCa}}{s_{\text{HPQC\_rated}}} \right)^2} \\
k_{\text{invaLC\_min}} \le k_{\text{invaLC}} \le k_{\text{invaLC\_max}}
\end{cases}
\tag{19}
$$

The railway HPQC compensation capability can then be determined by solving (19). Assuming that the load power factor is PF_L, the boundary condition of railway HPQC compensation capability is manipulated as follows:

$$
r_{\max} = \left(\frac{s_{\text{HPQC\_rated}}}{s_{L\_\text{rated}}} \right)
$$
$$
\cdot \left(\frac{\dfrac{M}{\sqrt{M^2+1}} + \sqrt{\dfrac{M^2}{M^2+1} - \left(1 - k_{\text{invaLC}}^2 \right)}}{m_{LCa}} \right)
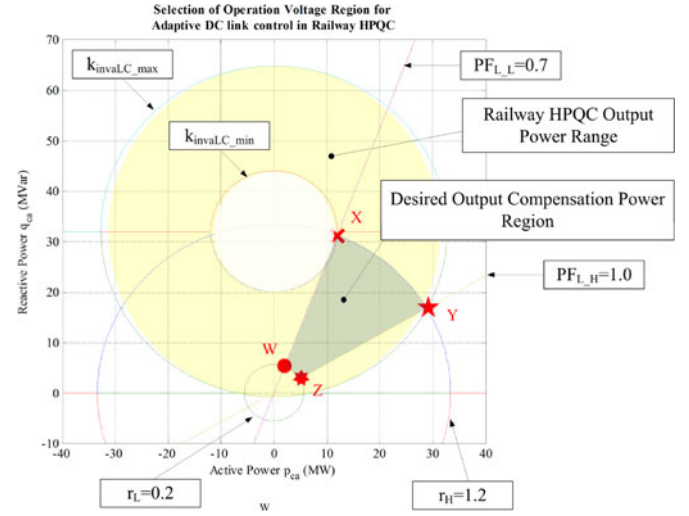$$

Fig. 11. MATLAB plot showing the railway HPQC output power range covering the desired output compensation power region (satisfactory compensation performance can be provided).

$$
r_{\min} = \left(\frac{s_{\text{HPQC\_rated}}}{s_{L\_\text{rated}}} \right)
$$
$$
\cdot \left(\frac{\dfrac{M}{\sqrt{M^2+1}} - \sqrt{\dfrac{M^2}{M^2+1} - \left(1 - k_{\text{invaLC}}^2 \right)}}{m_{LCa}} \right).
\tag{20}
$$

IV. OPERATION RANGE FOR FLEXIBLE DC VOLTAGE CONTROL IN RAILWAY HPQC

Based on the earlier discussions, the operation voltage range for flexible dc voltage control can be determined. Shown in Fig. 11 is a MATLAB plot illustrating the selection of the operation voltage range. It can be seen as a combination of Fig. 7 (railway HPQC output power range) and Fig. 10 (railway HPQC required compensation power). The railway HPQC output power range is defined by the upper circles [center not at (0, 0)].

Satisfactory compensation performance can be obtained only when the railway HPQC output power range covers the desired output region. Suppose that the larger upper circle is developed by the operation voltage $k_{\text{invaLC\_}H}$ while the smaller one is developed by the operation voltage k_{invaLC_L} and the four boundary points of the required railway HPQC output compensation power are the points X, Y, W, and Z. It is further supposed that the load capacity varies from r_L to r_H, while the load power factor varies from PF_{L_L} to PF_{L_H}. The corresponding railway HPQC rating of the intersection points W, X, Y, Z are defined as $k_{\text{invaLC\_}W}$, $k_{\text{invaLC\_}X}$, $k_{\text{invaLC\_}Y}$, and $k_{\text{invaLC\_}Z}$, as shown in (21), which is manipulated by substituting the railway HPQC required compensation power in (16) into (8), eq. (21) shown at the bottom of the next page, where $m_{\text{pq}L} = \left\{ \frac{2 \cdot [0.2887(\text{PF}_{L\_L}) + \sqrt{1 - (\text{PF}_{L\_L})^2}]}{\text{PF}_{L\_L}} \right\}$ and $m_{\text{pq}H} = \left\{ \frac{2 \cdot [0.2887(\text{PF}_{L\_H}) + \sqrt{1 - (\text{PF}_{L\_H})^2}]}{\text{PF}_{L\_H}} \right\}$.

Based on the earlier expressions, the upper range and the lower range of the railway HPQC operation voltage can then be

determined using (22)

$$\begin{cases} k_{\text{invaLC\_}L} = \min(W, X, Y, Z) \\ k_{\text{invaLC\_}H} = \max(W, X, Y, Z) \end{cases}. \tag{22}$$

With the operation voltage rating k_{invaLC} as the rms value of the railway HPQC voltage output, the dc voltage would signify the peak value so that (22) can be further manipulated as (23)

$$\begin{cases} V_{dc\_L} = \sqrt{2} \cdot k_{\text{invaLC\_}L} \\ V_{dc\_H} = \sqrt{2} \cdot k_{\text{invaLC\_}H} \end{cases}. \tag{23}$$

V. CONTROL BLOCK DIAGRAM OF RAILWAY HPQC WITH FLEXIBLE DC VOLTAGE CONTROL

Based on the earlier analysis, the control block diagram of railway HPQC with flexible dc voltage control is shown in Fig. 12. They are mainly composed of these computation blocks:

1) Single-phase instantaneous PQ computation blocks: To compute the required compensation power.
2) DC voltage control block: In addition to the required compensation power, additional active power is absorbed or emitted to control the dc voltage as the referenced level.
3) DC voltage reference determination block: There must be a reference dc voltage level in order to complete the flexible dc voltage control. The reference level is computed based on railway HPQC active and reactive power output requirement.
4) V_{dc}^* selection block: This is a sub-block in the dc voltage reference determination block. It is mainly used to determine which level the reference voltage should be located at since rapid changes in dc operation voltage may degrade the compensation performance.
5) Compensation current reference computation blocks: This control block is used to compute the reference output current signal according to the compensation power and voltage control requirement.
6) PWM general blocks: In order to control the railway HPQC to output required compensation current, this control block is required to generate the trigger signal
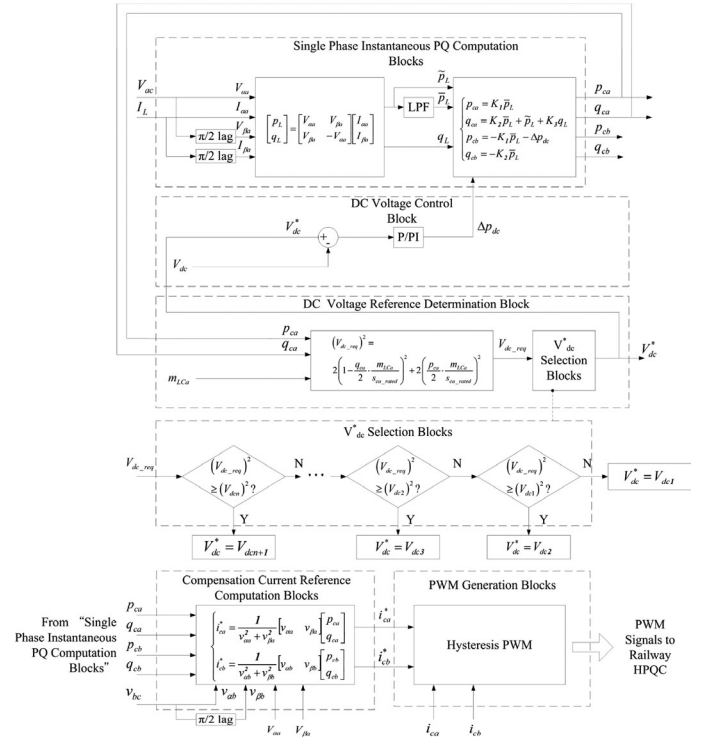

Fig. 12. Control block diagram of railway HPQC with proposed flexible dc voltage control to provide power quality compensation in co-phase traction power supply.

to the electronic switches (IGBT in this case) of railway HPQC.

Details of each control block will be explained later.

A. Single-Phase Instantaneous PQ Computation Blocks

First, the instantaneous load active and reactive power is computed using instantaneous *pq* theory proposed by Akagi *et al.* [27], with certain modification for single-phase computation

$$k_{\text{invaLC\_}W} = \sqrt{\left(1 - (m_{\text{pq}L})\left(\frac{r_L \cdot m_{\text{LC}a}}{\sqrt{1 + (m_{\text{pq}L})^2}}\right)\right)^2 + \frac{(r_L \cdot m_{\text{LC}a})^2}{\sqrt{1 + (m_{\text{pq}L})^2}}}$$

$$k_{\text{invaLC\_}X} = \sqrt{\left(1 - (m_{\text{pq}L})\left(\frac{r_H \cdot m_{\text{LC}a}}{\sqrt{1 + (m_{\text{pq}L})^2}}\right)\right)^2 + \frac{(r_H \cdot m_{\text{LC}a})^2}{\sqrt{1 + (m_{\text{pq}L})^2}}}$$

$$k_{\text{invaLC\_}Y} = \sqrt{\left(1 - (m_{\text{pq}H})\left(\frac{r_H \cdot m_{\text{LC}a}}{\sqrt{1 + (m_{\text{pq}H})^2}}\right)\right)^2 + \frac{(r_H \cdot m_{\text{LC}a})^2}{\sqrt{1 + (m_{\text{pq}H})^2}}}$$

$$k_{\text{invaLC\_}Z} = \sqrt{\left(1 - (m_{\text{pq}H})\left(\frac{r_H \cdot m_{\text{LC}a}}{\sqrt{1 + (m_{\text{pq}H})^2}}\right)\right)^2 + \frac{(r_H \cdot m_{\text{LC}a})^2}{\sqrt{1 + (m_{\text{pq}H})^2}}} \tag{21}$$

application, as shown in (24)

$$\begin{bmatrix} p_L \\ q_L \end{bmatrix} = \begin{bmatrix} v_{\alpha a} & v_{\beta a} \\ v_{\beta a} & -v_{\alpha a} \end{bmatrix} \begin{bmatrix} i_{\alpha a} \\ i_{\beta a} \end{bmatrix}$$

$$= \begin{bmatrix} v_{\mathrm{ac}} & v_{\mathrm{ac}} e^{-j\pi/2} \\ v_{\mathrm{ac}} e^{-j\pi/2} & -v_{\mathrm{ac}} \end{bmatrix} \begin{bmatrix} i_L \\ i_L e^{-j\pi/2} \end{bmatrix}. \qquad (24)$$

The required output compensation power of railway HPQC is then computed based on (25), in which a component Δp_{dc} is added compared to (11) for the dc voltage control and will be explained soon

$$\begin{cases} p_{\mathrm{ca}} = K_1 \bar{p}_L \\ q_{\mathrm{ca}} = K_2 \bar{p}_L + \tilde{p}_L + K_3 q_L \\ p_{\mathrm{cb}} = -K_1 \bar{p}_L - \Delta p_{\mathrm{dc}} \\ q_{\mathrm{cb}} = -K_2 \bar{p}_L \end{cases}. \qquad (25)$$

B. DC Voltage Control Blocks

The dc voltage control block is one important part. It is mainly used to allow the dc voltage V_{dc} of the railway HPQC vary according to the voltage reference V_{dc}^* in order to provide sufficient voltage for satisfactory power quality compensation in co-phase traction power supply system. This is accomplished mainly by P or PI controller, and its main function is shown in (26)

$$\Delta p_{\mathrm{dc}} = \left(k_p + \frac{k_I}{s} \right) \left(V_{\mathrm{dc}}^* - V_{\mathrm{dc}} \right). \qquad (26)$$

Referring to (25), the part Δp_{dc} is added as additional active power absorption into railway HPQC via V_{bc} phase converter. The value of Δp_{dc} varies with the error between the actual dc voltage and reference one to provide feedback to the system for dc voltage control. Next, the dc voltage reference determination is being discussed.

C. DC Voltage Reference Determination Blocks

The dc voltage reference is mainly determined by the operation voltage requirement, as derived in (8). In order to avoid the computation of square root in the processing unit (DSP), the determination is further manipulated as in (27). Notice that the instantaneous power is divided by two in order to compute traditional active and reactive power

$$(V_{\mathrm{dc\_req}})^2 = 2 \left(1 - \frac{q_{\mathrm{ca}}}{2} \cdot \frac{m_{\mathrm{LC}a}}{s_{\mathrm{ca\_rated}}} \right)^2 + 2 \left(\frac{p_{\mathrm{ca}}}{2} \cdot \frac{m_{\mathrm{LC}a}}{s_{\mathrm{ca\_rated}}} \right)^2. \qquad (27)$$

The computed value of $(V_{\mathrm{dc\_req}})^2$ will then be passed through dc voltage reference selection blocks to determine the value of V_{dc}^*.

D. DC Voltage Reference Determination Blocks

As mentioned earlier, the dc voltage reference V_{dc}^* is selected based on the dc voltage requirement $V_{\mathrm{dc\_req}}$. Ideally, the dc voltage reference may be the same as the railway HPQC dc voltage requirement $V_{\mathrm{dc\_req}}$; however, the dc voltage reference may vary during small load variations or measurement error; this

would cause frequent fluctuations in the dc voltage and make the compensation performance unstable. Therefore, a flexible dc voltage control method is adopted such that there will be different levels for the dc voltage reference such that the dc voltage of railway HPQC will be adaptively changed to these reference levels according to the requirement.

The range of dc operation voltage is discussed in Section IV, and the corresponding upper and lower boundary levels, $V_{\mathrm{dc_L}}$ and $V_{\mathrm{dc_H}}$, are defined as in (21), (22), and (23). The dc operation voltage range is then divided into N levels such that different railway HPQC operation voltage level $V_{\mathrm{dc}n}$ is defined in (28)

$$V_{\mathrm{dc}n} = V_{\mathrm{dc\_L}} + (n - 1) \cdot \left(\frac{V_{\mathrm{dc\_H}} - V_{\mathrm{dc\_L}}}{N} \right),$$
$$\text{for } 1 \le n \le N + 1. \qquad (28)$$

The selection of dc-link voltage reference V_{dc}^* is then performed based on (29). In short, the value of V_{dc}^* is selected as the nearest level, which is larger than the required dc voltage $V_{\mathrm{dc\_req}}$

$$\text{if } (V_{\mathrm{dc\_req}})^2 \ge (V_{\mathrm{dc}N})^2 \Rightarrow V_{\mathrm{dc}}^* = V_{\mathrm{dc}N+1}$$
$$\text{else if } (V_{\mathrm{dc\_req}})^2 \ge (V_{\mathrm{dc}N-1})^2 \Rightarrow V_{\mathrm{dc}}^* = V_{\mathrm{dc}N}$$
$$\cdots$$
$$\text{else if } (V_{\mathrm{dc\_req}})^2 \ge (V_{\mathrm{dc}2})^2 \Rightarrow V_{\mathrm{dc}}^* = V_{\mathrm{dc}3}$$
$$\text{else if } (V_{\mathrm{dc\_req}})^2 \ge (V_{\mathrm{dc}1})^2 \Rightarrow V_{\mathrm{dc}}^* = V_{\mathrm{dc}2}$$
$$\text{else } \Rightarrow V_{\mathrm{dc}}^* = V_{\mathrm{dc}1}. \qquad (29)$$

E. Compensation Current Reference Computation and PWM Generation Blocks

Since the final goal of the railway HPQC is to output the required compensation current in order to provide satisfactory compensation performance, it is important to transform the compensation power into compensation current reference. This is done so by taking the inverse transform, as shown in (30)

$$\begin{cases} i_{\mathrm{ca}}^* = \dfrac{1}{v_{\alpha a}^2 + v_{\beta a}^2} \begin{bmatrix} v_{\alpha a} & v_{\beta a} \end{bmatrix} \begin{bmatrix} p_{\mathrm{ca}} \\ q_{\mathrm{ca}} \end{bmatrix} \\ i_{\mathrm{cb}}^* = \dfrac{1}{v_{\alpha b}^2 + v_{\beta b}^2} \begin{bmatrix} v_{\alpha b} & v_{\beta b} \end{bmatrix} \begin{bmatrix} p_{\mathrm{cb}} \\ q_{\mathrm{cb}} \end{bmatrix} \end{cases} \qquad (30)$$

where i_{ca}^* is the V_{ac} phase converter compensation current reference, while i_{cb}^* is the V_{bc} phase converter compensation current reference of railway HPQC.

This compensation current reference is compared with the actual output compensation current i_{ca} and i_{cb}, in order to generate PWM signals using hysteresis PWM operating at linear region [32]. The PWM signals are then sent to the electronic switches of railway HPQC to control the compensation operation and power flow.

VI. SIMULATION VERIFICATIONS

In order to verify the effects of operation voltage range in flexible dc-link voltage control on railway HPQC compensation

TABLE I
DETERMINATION FOR DC OPERATION VOLTAGE RANGE IN RAILWAY HPQC OF
CO-PHASE TRACTION FOR LOAD VARIATIONS

No.	Parameters	Symbol	Value
1.	Minimum load capacity	r_A	0.2
2.	Maximum load capacity	r_B	1.2
3.	Lower load power factor	PF_{L_L}	0.7
4.	Higher load power factor	PF_{L_H}	1.0
5.	Lower dc-link operation voltage	V_{dc_L}	14.5 kV
6.	Higher dc-link operation voltage	V_{dc_H}	39.8 kV
7.	DC-link operation voltage interval	$V_{dc\_interval}$	8.4 kV

TABLE II
SYSTEM PARAMETERS USED IN THE SIMULATION VERIFICATION OF RAILWAY
HPQC USING FLEXIBLE DC-LINK VOLTAGE CONTROL FOR LOAD VARIATIONS

No.	Parameters	Symbol	Value
1.	V_{ac} phase-coupled impedance ratio	m_{LCa}	0.8761
2.	V_{ac} phase-coupled inductance ratio	k_L	0.0912
3.	V_{ac} phase-coupled inductance	L_a	6.5 mH
4.	V_{ac} phase-coupled capacitance	C_a	131 μF
5.	V_{bc} phase-coupled inductance	L_b	6 mH
6.	DC-link capacitance	C_{DC}	10 000 μF
7.	DC-link operation voltage range	V_{dc}	14.5–39.8 kV

performance in co-phase traction power supply, simulations are done using PSCAD. The circuit schematic is similar to the one in Fig. 4. The system source grid is 220 kV, and the traction load is electrified with 27.5 kV. It is further assumed that the traction load capacity variation range is from 0.2 to 1.2 p.u., while the traction power factor variation range is from 0.7 to 1.0. The dc operation voltage range of railway HPQC with flexible dc voltage control is derived based on the analysis throughout this paper, and the results are presented in Table I. The railway HPQC system parameters are selected based on nominal rated load [19] ($\mathrm{PF}_L = 0.85$, rated load capacity = 31 MVA) and is shown in Table II.

The value of m_{LCa} can be chosen based on different requirements such as operation voltage or compensation range concern. For example, the value selected here is calculated based on the minimum operation voltage requirement in railway HPQC at a rated designed load [19]. The expression for capacitance determination is presented in (31)

$$C_a = \frac{1}{\omega X_{LCa}} = \frac{I_{ca\_rated}}{\omega V_{ac} \cdot \sin\theta_{ca\_rated}}. \tag{31}$$

For the value of k_L, it is calculated based on the concern of minimum operation voltage under harmonic compensation [20]. The main equation for the derivation of k_L is shown in (32)

$$k_L = \frac{\sum_{h=2}^{\infty}(r_h)^2 \cdot \frac{2(h^2-1)}{h^2}}{\sum_{h=2}^{\infty}(r_h)^2 \cdot \frac{2(h^2-1)^2}{h^2}} \tag{32}$$

where r_h is the ratio of the hth harmonic order load current to the fundamental load current and h is the multiple ratio of the fundamental frequency (hth harmonic order)
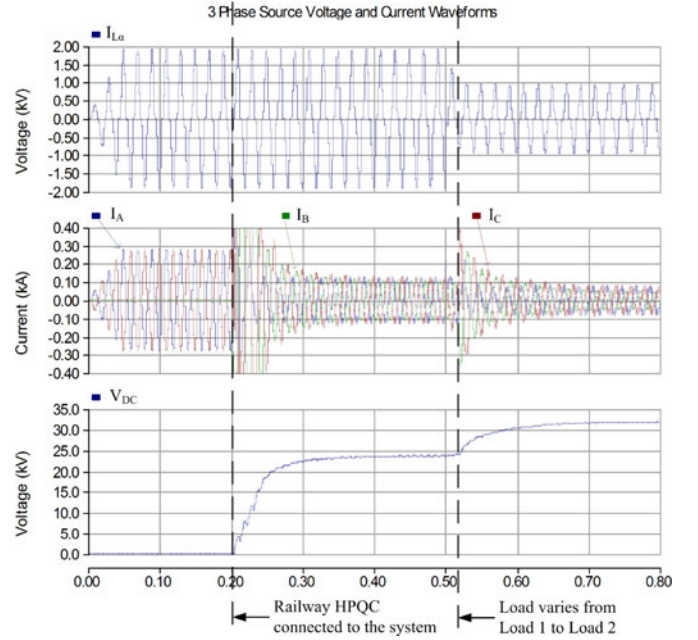

Fig. 13. Simulated load current, source current and dc-link voltage waveforms for railway HPQC with proposed flexible dc-link voltage control.
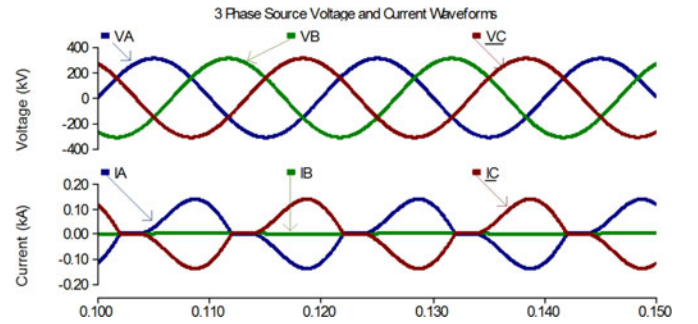

Fig. 14. Simulated system source voltage and current waveforms without any compensation.

A. Overall Performance

In the simulation, the railway HPQC is connected to the system at 0.2 s, while the load is varied from Load 1 ($\mathrm{PF}_L = 0.85$, $r = 1.0$ p.u.) to Load 2 ($\mathrm{PF}_L = 0.85$, $r = 0.5$ p.u.) at 0.51 s. The simulated waveforms obtained are shown in Fig. 13.

It can be observed that when loading condition is changed at 0.51 s, the dc voltage of the railway HPQC is adaptively changed from 23.5 to 32 kV in order to provide satisfactory compensation performance. By doing so, the dc link voltage can operate at a lower level (if applicable) during load variations to reduce switching loss and ripples.

B. Without Compensation (Time < 0.2 s)

The simulated waveforms of system source voltage and current without compensation (time < 0.2 s) is shown in Fig. 14. It can be observed that at 0.51s, the loading condition is changed, at the same time the dc voltage of the railway HPQC is also
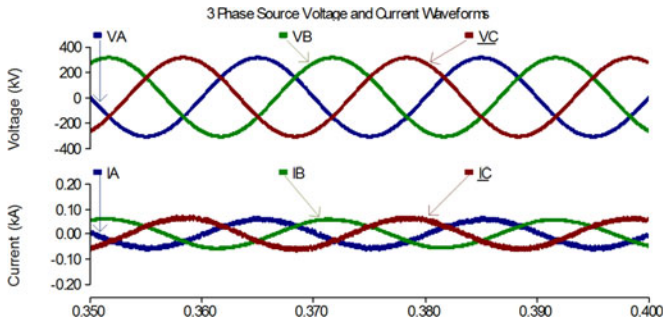
Fig. 15.   Simulated system source voltage and current waveforms with railway HPQC Compensation under Load 1 (rated load, 1.0 p.u.) (railway HPQC connected to the system at 0.2 s).
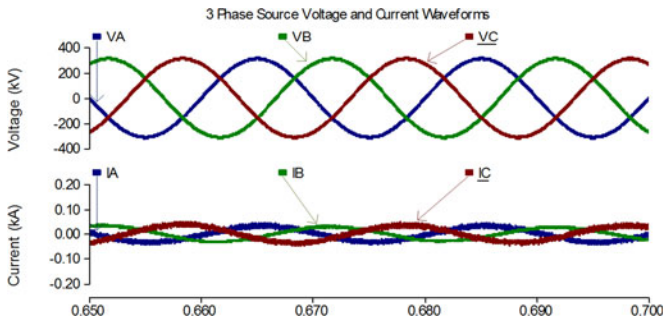

Fig. 16.   Simulated system source voltage and current waveforms with railway HPQC compensation under Load 2 (half-rated load, 0.5 p.u.) (switched into the system at 0.51 s).

adaptively changed from 23.5 to 32 kV in order to provide satisfactory compensation performance.

C. Railway HPQC Connected Under Load 1 (0.2 s < Time < 0.51 s)

At time $t = 0.2$ s, the railway HPQC is connected to the system to provide power quality compensation. The simulated waveforms obtained are shown in Fig. 15. It can be seen that compared to Fig. 14, the system source current is balanced and harmonic-free. Referring to Fig. 13, the dc-link voltage is 23.5 kV.

D. Load 1 Changed to Load 2 (Time > 0.51 s)

At time $t = 0.51$ s, the load is changed from Load 1 to Load 2, in which larger active power is required to be output by railway HPQC. The simulated waveforms are shown in Fig. 16. It can be seen that the system source current is balanced, and the harmonics are eliminated. The system source power factor is 0.99, the system source current harmonic distortions is 2.69%, and the system source current unbalanced is 13.32%, which is also within the performance standard. Similarly, referring to Fig. 13, the dc voltage of railway HPQC is 32 kV. The dc voltage is adaptively changed to another level when the loading condition is changed.

In order to show clearly the system performance, the detailed power quality data, namely, the system source power factor, the source current total harmonic distortions, and the system

TABLE III
SIMULATED SYSTEM PERFORMANCE DATA FOR THE FLEXIBLE DC-LINK
VOLTAGE CONTROL VERIFICATIONS

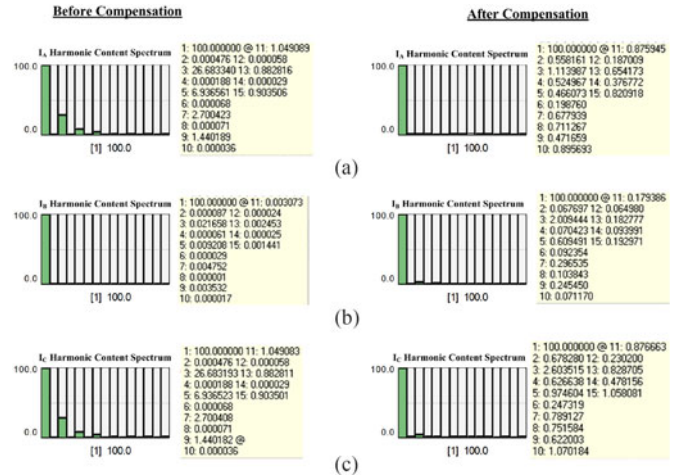|	V^*_{dc}	V_{dc}	PF	THD (%)	I_{un} (%)
Without compensation (Before 0.2 s)	–	–	0.60	27.78	99
Load 1 (1.0 p.u.) (0.2 to 0.5 s)	23.3 kV	23.5 kV	0.99	3.15	6.80
Load 2 (0.5 p.u.) (After 0.5 s)	31.5 kV	32 kV	0.99	2.69	13.32

Fig. 17.   Harmonic content spectrum of source current before and after compensation: (a) I_A, (b) I_B, and (c) I_C.

unbalance, are shown in Table III. It can be shown that using railway HPQC with proposed flexible dc voltage control, the dc voltage can be adaptively changed according to the dc voltage reference based on the loading condition in order to reduce the switching loss during operation.

For reference, the harmonic content spectrum of the three phase source current I_A, I_B I_C are shown in Fig. 17. The compensation performance is evaluated using the IEEE Standard 519-1992, "IEEE Recommended Practices and Requirements for Harmonic Control in Electrical Power Systems" [33]. Based on the information, for a 220-kV system, as in the condition being investigated, the total harmonic distortions should be less than 3.5%, with individual harmonic content less than 3.0%. It is shown through the results that the performance satisfy the standard.

E. Comparisons with Fixed DC Operation Voltage Control Method

In order to do further comparisons, the simulations are done with fixed dc-link voltage control, at around 32 kV. The captured waveforms are shown in Fig. 18. The simulated performance is also presented in Table IV. Comparing the data with Table III, it can be observed that the system performance of railway HPQC using flexible dc operation voltage control is similar to the fixed dc one. However, the operation voltage can be reduced under Load 1 condition to reduce the switching loss.
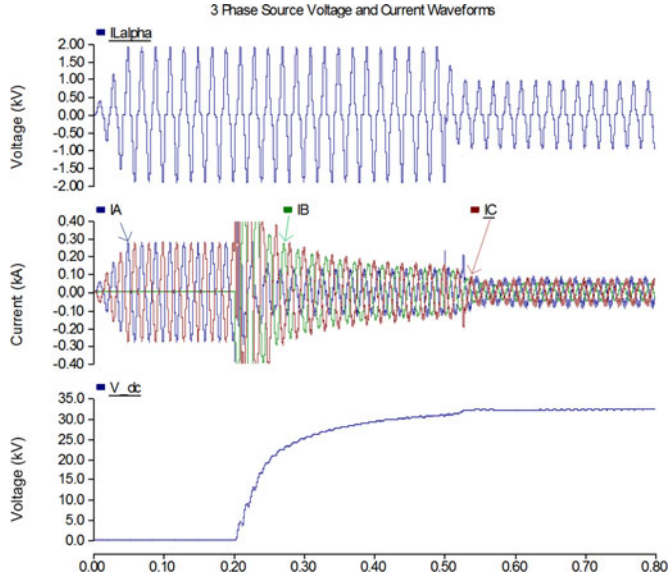
Fig. 18. Simulated load current, source current, and dc-link voltage waveforms for railway HPQC with fixed dc-link voltage control ($V_{dc}^* = 32$ kV).

TABLE IV
SIMULATED SYSTEM PERFORMANCE DATA FOR THE FIXED
DC-LINK VOLTAGE CONTROL

	V_{dc}	PF	THD (%)	I_{un} (%)
Without compensation (Before 0.2 s)	–	0.60	27.78	99
Load 1 (1.0 p.u.) (0.2 to 0.5 s)	32 kV	0.98	2.98	14.30
Load 2 (0.5 p.u.) (after 0.5 s)	32 kV	0.99	2.70	13.50
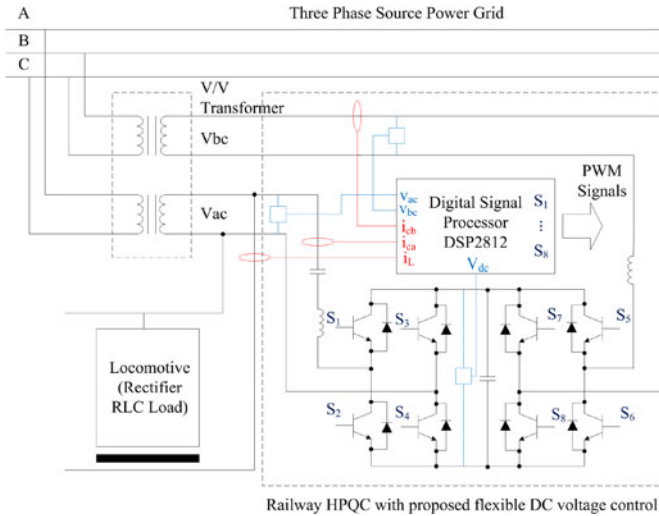
Fig. 19. Schematics of the hardware prototype of co-phase with railway HPQC using flexible dc voltage control.

VII. HARDWARE PROTOTYPE AND EXPERIMENTAL RESULTS

A hardware prototype of co-phase traction power supply with railway HPQC is constructed at laboratory level to obtain experimental results for verifications. The hardware schematics of the hardware prototype is shown in Fig. 19. For safety

Fig. 20. Hardware appearance of laboratory-scaled hardware prototype of co-phase supply with railway HPQC.

TABLE V
EXPERIMENTAL CIRCUIT PARAMETER OF RAILWAY HPQC USING PROPOSED
FLEXIBLE DC VOLTAGE CONTROL

No.	Parameters	Symbol	Value
1.	V_{ac} phase-coupled impedance ratio	m_{LCa}	0.876
2.	V_{ac} phase-coupled inductance ratio	k_L	0.10
3.	V_{ac} phase-coupled inductance	L_a	4.9 mH
4.	V_{ac} phase-coupled capacitance	C_a	170 μF
5.	V_{bc} phase-coupled inductance	L_b	4 mH
6.	DC-link capacitance	C_{dc}	10 000 μF
7.	DC operation voltage range	V_{dc}	26–72 V
8.	Number of intervals in the operation voltage range	n	3
9.	DC-link voltage levels	V_{dcn}	26 V
			41.7 V
			57 V
			72 V

concerns and preliminary analysis, the voltage is reduced with a ratio of 1:550, with the load voltage of 50 V. The control unit used is DSP2812. The voltage of two V/V traction transformer secondary outputs (V_{ac}, V_{bc}), the traction load current (i_L) are measured to compute the required railway HPQC compensation active and reactive power as well as the dc voltage level according to the derivations and analysis in this paper. The compensation current is then generated by comparing the actual one and the reference one to provide feedback for hysteresis PWM control while the actual dc voltage V_{dc} is also measured for flexible dc voltage control. More details can be found in Section VI.

The hardware appearance, with working bench and measuring instruments, is shown in Fig. 20. Detailed circuit parameter of railway HPQC using the proposed flexible dc voltage control is shown in Table V.

Experimental results are then obtained from the hardware prototype to verify the performance of the proposed flexible dc voltage control for railway HPQC. Similar to simulation verifications, the load is changed from one condition to another. Referring to the schematics in Fig. 19, the active and reactive power consumption of traction locomotive load is performed using the rectifier *RLC* load. The load condition is changed
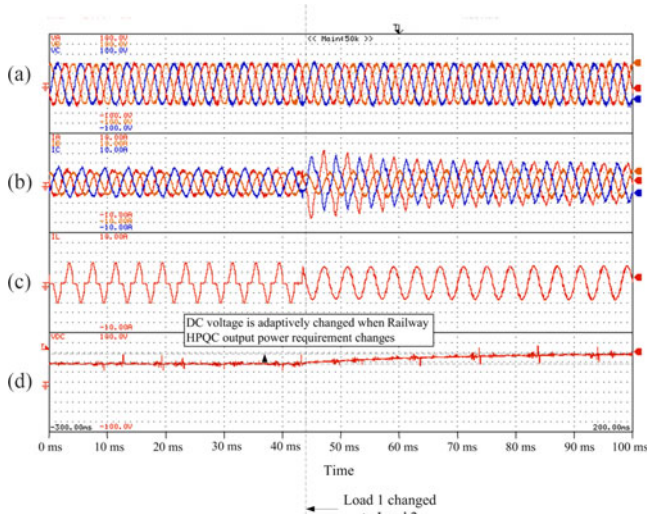
Fig. 21. Experimental waveforms obtained from the experiment: (a) three-phase system source voltage; (b) three-phase system source current; (c) load current; (d) dc voltage of railway HPQC.

from Load 1 ($r = 1.0$, $PF_L = 0.85$) to Load 2 ($r = 1.0$, $PF_L = 1.00$).

A. Overall Experiment Performance

The experimental waveforms obtained are shown in Fig. 21. It can be seen from the figure that when the load condition is changed from Load 1 to Load 2, the dc voltage of railway HPQC can be adaptively changed to another level when the output compensation power requirement of railway HPQC changes, i.e., when the load condition changes. More details about the system performance under different load conditions can be found later.

B. Load 1 ($V_{dc} = 41$ V)

During Load 1 condition, the dc voltage of railway HPQC is 41 V and the satisfactory compensation performance can be provided. The waveforms obtained during Load 1 are presented in Fig. 22.

The system source power factor is 0.96 and the source current harmonics is 8.9%, while the system source current unbalanced is 26.4%.

C. Load 2 ($V_{dc} = 72$ V)

When the load is changed from Load 1 to Load 2, the dc voltage of railway is adaptive changed from 41 to 72 V in order to provide satisfactory compensation performance according to the loading condition. The experimental waveforms obtained are shown in Fig. 23. During Load 2 condition, the system source power factor is 0.98, the system source current harmonics is 6.8%, and the system source current unbalanced is 22.2%.

The summary of the experimental results is shown in Table VI. It can be proved that by using proposed flexible dc voltage control, the dc voltage of railway HPQC can be changed according to the output compensation power requirement. By doing so, the
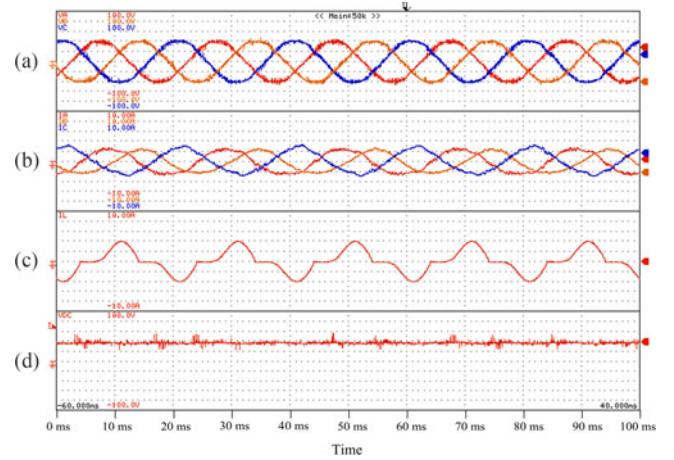

Fig. 22. Experimental waveforms obtained for Load 1: (a) three-phase source voltage; (b) three-phase source current; (c) load current; (d) dc voltage of railway HPQC ($V_{dc} = 41$ V).
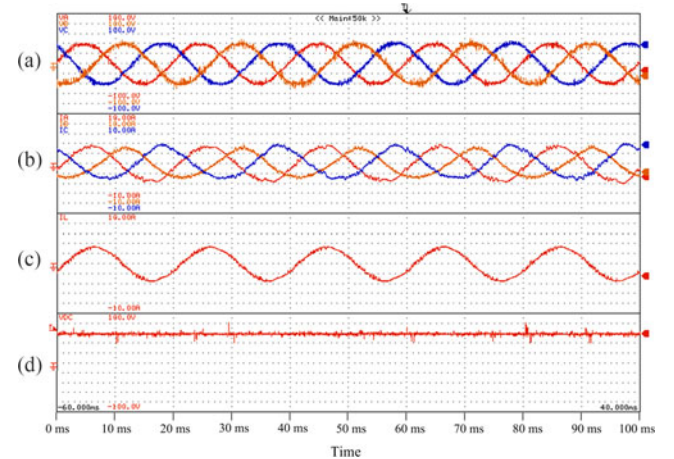

Fig. 23. Experimental waveforms obtained for Load 1: (a) three-phase source voltage; (b) three-phase source current; (c) load current; (d) dc voltage of railway HPQC ($V_{dc} = 72$ V).

TABLE VI
EXPERIMENTAL SYSTEM PERFORMANCE DATA FOR THE FLEXIBLE DC-LINK VOLTAGE CONTROL VERIFICATIONS

	V_{dc}^*	V_{dc}	PF	THD (%)	I_{un} (%)
Load 1 ($r = 1.0$, $PF_L = 0.70$)	41.2 V	41 V	0.96	8.9	26.4
Load 2 ($r = 1.0$, $PF_L = 1.00$)	72 V	72 V	0.98	6.8	22.2

dc operation voltage may be reduced during variations so that less switching and operation loss is consumed.

VIII. CONCLUSION

In conclusion, the effect of operation voltage range in flexible dc voltage control of railway HPQC on compensation performance is analyzed. First, the relationship between railway HPQC active and reactive power output capability and operation voltage range is modeled and analyzed. It is found that the railway HPQC active and reactive power output range is mainly

determined by the maximum value of the dc operation voltage range. Afterward, the effect of operation voltage range on railway HPQC compensation capability is analyzed and discussed. In order to evaluate the compensation capability, the changes in compensation requirement due to load capacity and power factor are explored. Based on the analysis earlier, the operation voltage range of flexible dc voltage control can then be determined. It is shown through simulation and experimental results that with the determined flexible dc voltage control operation range, railway HPQC can provide satisfactory compensation performance.

ACKNOWLEDGMENT

REFERENCES

[1] X. Sun, R. Han, H. Shen, B. Wang, Z. Lu, and Z. Chen, "A double-resistive active power filter system to attenuate harmonic voltages of a radial power distribution feeder," *IEEE Trans. Power Electron.*, vol. 31, no. 9, pp. 6203–6216, Sep. 2016.

[2] W. R. N. Santos *et al.*, "The transformerless single-phase universal active power filter for harmonic and reactive power compensation," *IEEE Trans. Power Electron.*, vol. 29, no. 7, pp. 3563–3572, Jul. 2014.

[3] P. Acuña, L. Morán, M. Rivera, J. Dixon, and J. Rodriguez, "Improved active power filter performance for renewable power generation systems," *IEEE Trans. Power Electron.*, vol. 29, no. 2, pp. 687–694, Feb. 2014.

[4] T.-L. Lee, J. C. Li, and P.-T. Cheng, "Discrete frequency tuning active filter for power system harmonics," *IEEE Trans. Power Electron.*, vol. 24, no. 5, pp. 1209–1217, May 2009.

[5] F. Z. Peng, G. W. Ott, and D. J. Adams, "Harmonic and reactive power compensation based on the generalized instantaneous reactive power theory for three-phase four-wire systems," *IEEE Trans. Power Electron.*, vol. 13, no. 6, pp. 1174–1181, Nov. 1998.

[6] S. M. M. Gazafrudi, A. T. Langerudy, E. F. Fuchs, and K. Al-Haddad, "Power quality issues in railway electrification: A comprehensive perspective," *IEEE Trans. Ind. Electron.*, vol. 62, no. 5, pp. 3081–3090, May 2015.

[7] *IEEE Recommended Practice and Requirements for Harmonic Control in Electric Power Systems, IEEE Std 519-2014 (Revision of IEEE Std 519-1992)*, 2014.

[8] *Quality of Electric Energy Supply Admissible Three Phase Voltage Unbalance*, National Standard GB/T 15543-2008.

[9] H. F. Brown and R. L. Witzke, "Shunt capacitor installation for single phase Railway service," *Trans. Amer. Inst. Electr. Eng.*, vol. 67, no. 1, pp. 258–266, 1948.

[10] G. Celli, F. Pilo, and S. B. Tennakoon, "Voltage regulation on 25 kV AC railway systems by using thyristor switched capacitor," in *Proc. 9th Int. Conf. Harmonics Qual. Power*, 2000, vol. 2, pp. 633–638

[11] P.-C. Tan, P. C. Loh, and D. G. Holmes, "A robust multilevel hybrid compensation system for 25-kV electrified railway applications," *IEEE Trans. Power Electron.*, vol. 19, no. 4, pp. 1043–1052, Jul. 2004.

[12] Q. Li, W. Liu, Z. Shu, S. Xie, and F. Zhou, "Co-phase power supply system for HSR," in *Proc. 2014 Int. Power Electron. Conf., IPEC-Hiroshima 2014—ECCE-ASIA*, 2014, pp. 1050–1053.

[13] Z. Shu *et al.*, "Digital detection, control, and distribution system for co-phase traction power supply application," *IEEE Trans. Ind. Electron.*, vol. 60, no. 5, pp. 1831–1839, May 2013.

[14] Z. Shu, S. Xie, and Q. Li, "Single-phase back-to-back converter for active power balancing, reactive power compensation, and harmonic filtering in traction power system," *IEEE Trans. Power Electron.*, vol. 26, no. 2, pp. 334–343, Feb. 2011.

[15] Z. Shu, S. Xie, and Q. Li, "Single-phase back-to-back converter for active power balancing, reactive power compensation, and harmonic filtering in traction power system," *IEEE Trans. Power. Electron.*, vol. 26, no. 2, pp. 334–343, Feb. 2011.

[16] Z. Shu, S. Xie, and Q.-z. Li, "Development and implementation of a prototype for co-phase traction power supply system," in *Proc. Power Energy Eng. Conf., APPEEC, Asia-Pacific*, 2010, pp. 1–4.

[17] M. Chen, Q.-z. Li, and G. Wei, "Optimized design and performance evaluation of new cophase traction power supply system," in *Proc. Power Energy Eng. Conf., APPEEC, Asia-Pacific*, 2009, pp. 1–6.

[18] N. Y. Dai, K. W. Lao, M. C. Wong, and C. K. Wong , "Hybrid power quality conditioner for co-phase power supply system in electrified railway," *IET Power Electron.*, vol. 5, no. 7, pp. 1084–1094, 2012.

[19] K.-W. Lao, N. Dai, W.-G. Liu, and M.-C. Wong, "Hybrid power quality compensator with minimum DC operation voltage design for high-speed traction power systems," *IEEE Trans Power Electron.*, vol. 28, no. 4, pp. 2024–2036, Apr. 2013.

[20] K.-W. Lao, M.-C. Wong, N. Dai, C.-K. Wong, and C.-S. Lam, "A systematic approach to hybrid railway power conditioner design with harmonic compensation for high-speed railway," *IEEE Trans. Ind. Electron.*, vol. 62, no. 2, pp. 930–942, Feb. 2015.

[21] K.-W. Lao, M.-C. Wong, N. Dai, C.-K. Wong, and C.-S. Lam, "Analysis of DC link operation voltage of a hybrid railway power quality conditioner and its PQ compensation capability in high speed co-phase traction power supply," *IEEE Trans. Power Electron.*, vol. 31, no. 2, pp. 1643–1656, Feb. 2016.

[22] N. Dai, K. Lao, and C. Lam, "Hybrid railway power conditioner with partial compensation for rating optimization," *IEEE Trans. Ind. Appl.*, vol. 51, no. 5, pp. 4130–4138, Sep.-Oct. 2015.

[23] N.-Y. Dai, M.-C. Wong, K.-W. Lao, and C.-K. Wong, "Modelling and control of a railway power conditioner in co-phase traction power system under partial compensation," *IET Power Electron.*, vol. 7, no. 5, pp. 1044–1054, May 2014.

[24] K.-W. Lao, N. Dai, W. Liu, M.-C. Wong, and C. K. Wong, "Modeling and control of railway static power conditioner compensation based on power quality standards," in *Proc. IEEE 13th Workshop Control Model. Power Electron.*, pp. 1–6, 2012.

[25] F. Wu, B. Li, and J. Duan, "Calculation of switching loss and current total harmonic distortion of cascaded multilevel grid-connected inverter and Europe efficiency enhancement considering variation of DC source power," *IET Power Electron.*, vol. 9, no. 2, pp. 336–343, 2016.

[26] C.-S. Lam, M.-C. Wong, W.-H. Choi, X.-X. Cui, H.-M. Mei, and J.-Z. Liu, "Design and performance of an adaptive low-DC-voltage-controlled LC-hybrid active power filter with a neutral inductor in three-phase four-wire power systems," *IEEE Trans. Ind. Appl.*, vol. 61, no. 6, pp. 2635–2647, Jun. 2014.

[27] H. Akagi, Y. Kanazawa, and A. Nabae, "Instantaneous reactive power compensators comprising switching devices without energy storage components," *IEEE Trans. Ind. Appl.*, vol. IA-20, no. 3, pp. 625–630, May 1984.

[28] A. Luo, F. Ma, C. Wu, S. Q. Ding, Q.-C. Zhong, and Z. K. Shuai, "A dual-loop control strategy of railway static power regulator under V/V electric traction system," *IEEE Trans. Power Electron.*, vol. 26, no. 7, pp. 2079–2091, Jul. 2011.

[29] A. Luo, C. Wu, J. Shen, Z. Shuai, and F. Ma, "Railway static power conditioners for high-speed train traction power supply systems using three-phase V/V transformers," *IEEE Trans. Power Electron.*, vol. 26, no. 10, pp. 2844–2856, Oct. 2011.

[30] S. Hu *et al.*, "A new railway power flow control system coupled with asymmetric double LC branches," *IEEE Trans. Power Electron.*, vol. 30, no. 10, pp. 5484–5498, Oct. 2015.

[31] D. Zhang, Z. Zhang, W. Wang, and Y. Yang, "Negative sequence current optimizing control based on Railway static power conditioner in V/v traction power supply system," *IEEE Trans. Power Electron.*, vol. 31, no. 1, pp. 200–212, Jan. 2016.

[32] C.-S. Lam, M.-C. Wong, and Y.-D. Han, "Hysteresis current control of hybrid active power filters," *IET Power Electron.*, vol. 5, no. 7, pp. 1175–1187, Aug. 2012.

[33] *IEEE Recommended Practices and Requirements for Harmonic Control in Electrical Power Systems*, IEEE Standard 519-1992.

Keng-Weng Lao (S'09–M'17) was born in Macau, China, in 1987. He received the B.Sc., Master's, and Ph.D. degrees in the electrical and electronics engineering from the Faculty of Science and Technology, University of Macau, Macao, in 2009, 2011, and 2016, respectively.

He is currently a Lecturer in the Department of Electrical and Computer Engineering, University of Macau. His current research interests include FACTS compensation devices, renewable energy, energy saving, and energy management.

Dr. Lao was the recipient of the Macao Science and Technology Development Fund—Postgraduate Award for Ph.D. Student 2016. He was also the first runner-up of the Challenge Cup National Inter-varsity Science and Technology Competition, and Championship of the Postgraduate Section in the IET Young Professionals Exhibition and Competition in China and Hong Kong, respectively, in 2013. He also received the Champion Award of the Schneider Electric Energy Efficiency Cup in Hong Kong in 2010. He was secretary and Publication Chair of the conference IEEE TENCON 2015.

Man-Chung Wong (SM'06) received the B.Sc. and M.Sc. degrees in electrical and electronics engineering from the Faculty of Science and Technology, University of Macau, Macao, China, in 1993 and 1997 respectively, and the Ph.D degree from Tsinghua University, Beijing, China, in 2003.

Since 2008, he has been an Associate Professor at the University of Macau. His current research interests include FACTS and DFACTS, power quality, custom power, and PWM.

Dr. Wong received the Young Scientist Award from the "Instituto Internacional De Macau" in 2000, the Young Scholar Award from the University of Macau in 2001, the second prize of 2003 Tsinghua University Excellent Ph.D. Thesis Award, and the third prize of 2012 Macao Technology Invention Award given by Macao Science and Technology Fund (FDCT).
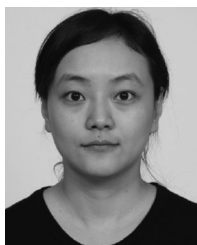
NingYi Dai (S'05–M' 08–SM'15) was born in Jiangsu, China, in 1979. She received the B.Sc. degree in electrical engineering from the Southeast University, Nanjing, China, in 2001, and the M.Sc. and Ph.D. degrees in electrical and electronics engineering from the Faculty of Science and Technology, University of Macau, Macao, China, in 2004 and 2007, respectively.

She is currently an Associate Professor in the Department of Electrical and Computer Engineering, University of Macau. She has authored or coauthored more than 70 technical journals and conference papers in the field of power system and power electronics. Her current research interests include application of power electronics in power system, renewable energy integration, and flexible dc distribution system.

Dr Dai was the co-recipient of the Macao Science and Technology Invention Award (Third-Class) in 2012.

Chi-Seng Lam (S'04–M'12–SM'16) received the B.Sc., M.Sc., and Ph.D. degrees in electrical and electronics engineering from the University of Macau (UM), Macao, China, in 2003, 2006, and 2012 respectively.

From 2006 to 2009, he was an E&M Engineer in UM. In 2009, he simultaneously worked as a Laboratory Technician and started to pursue his Ph.D. degree. In 2013, he was a Postdoctoral Fellow in The Hong Kong Polytechnic University, Hong Kong, China. He is currently an Assistant Professor in the State Key Laboratory of Analog and Mixed-Signal VLSI, UM. He has coauthored 2 books *Design and Control of Hybrid Active Power Filters* (Springer, 2014) and *Parallel Power Electronics Filters in Three-phase Four-wire Systems - Principle, Control and Design* (Springer, 2016), 1 U.S. patent, 2 Chinese patents and over 60 technical journals and conference papers. His current research interests include integrated power electronics controllers, power management integrated circuits, power quality compensators, smart grid technology, renewable energy, etc.

Dr. Lam received the Macao Science and Technology Invention Award (Third-Class) and the R&D Award for Postgraduates (Ph.D.) in 2014 and 2012, respectively. He also received the Macao Government Ph.D. Research Scholarship in 2009–2012, the Macao Foundation Postgraduate Research Scholarship in 2003–2005, and the third RIUPEEEC Merit Paper Award in 2005. In 2007, 2008, and 2015, he was the GOLD Officer, Student Branch Officer, and Secretary of the IEEE Macau Section. He is currently the Vice-Chair of IEEE Macau Section, Chair of the IEEE Macau CAS&COM Joint Chapter, and Secretary of the IEEE Macau PES/PELS Joint Chapter. He was the Local Arrangement Chair of IEEE TENCON 2015 and ASP-DAC 2016.

Lei Wang received the B.Sc. degree in electrical and electronics engineering from the University of Macau (UM), Macao, China, in 2011, the M.Sc. degree in electronics engineering from Hong Kong University of Science and Technology (HKUST), Hong Kong, China, in 2012, and the Ph.D. degree in electrical and computer engineering from the UM in 2017.

He is currently a Postdoctoral Fellow in the Power Electronics Laboratory, UM. His current research interests include power electronics, power quality and distribution flexible ac transmission system (DFACTS), power quality compensation, and renewable energy.

Dr. Wang received the Champion Award in the "Schneider Electric Energy Efficiency Cup," Hong Kong, 2011.

Chi-Kong Wong (M'91) was born in Macao in 1968. He received the B.Sc. and M.Sc. degrees in electrical and electronics engineering (EEE) from the University of Macau, Macao, China, in 1993 and 1997, respectively, and the Ph.D. degree in EEE from Tsinghua University, Beijing, China, in 2007.

He was recruited by the University of Macau as a Teaching Assistant for the Faculty of Science and Technology in 1993 and promoted to the post of Lecturer and Assistant Professor in 1997 and 2008, respectively. Since 1997, he has been teaching the fundamental courses in the Department of Electrical and Electronics Engineering and supervising the final-year projects. In addition to the undergraduated teaching and supervision, he had also co-taught one master course and cosupervised three master research projects. His current research interests include voltage stability analysis, synchronized phasor measurement applications in power systems, wavelet transformation applications in power systems, renewable energy, power quality, and energy saving.

Dr. Wong received the third-class award in the Science and Technology Progress in 2012. He was the Vice Chair of the IEEE Macau in 2014 and Treasurer and Chair of Power Track of TENCON 2015.